Surface Flux Intercomparison Between the MM5 Model and Observations During the Storm-Scale Observations Regional Measurement Program-Fronts Experiment Systems Test 1992

J. Dudhia and S. P. Oncley
Mesoscale and Microscale Meteorology Division
Atmospheric Technology Division
National Center for Atmospheric Research
Boulder, Colorado

Introduction

Mesoscale model 5 (MM5) is being used as a data assimilation tool for the Atmospheric Radiation Measurement (ARM) Program. There is a need to verify that the model physics is consistent with observations under a range of conditions. Surface fluxes of heat, moisture, and momentum are a particular area of uncertainty in the model owing to their dependence on surface properties, some of which are time-dependent.

The National Center for Atmospheric Research (NCAR) Atmosphere-Surface Turbulent Exchange Research (ASTER) facility provides direct measurements of the fluxes near the surface by means of three-dimensional sonic anemometers collocated with fast-response temperature and humidity sensors. Additionally aircraft data from a low-flying King aircraft have been taken over the ASTER site.

Method and Objectives

The primary objective is to detect any systematic errors in the MM5 surface flux formulation that could have adverse effects on the model data assimilation and, thence, to suggest corrections that help avoid such inaccuracies.

Preliminary results of this intercomparison were reported last year for the Winter Icing and Storms Program 91 (WISP91) experiment in Colorado (Oncley and Dudhia 1993). Four simulations were run with MM5, corresponding to four days in the Storm-Scale Observations Regional Measurement Program-Fronts Experiment Systems Test '92 (STORM-FEST92) in which the King Air provided data over the ASTER site in northeast Kansas.

Model simulations of these days, initialized from 60-km Mesoscale Analysis and Prediction System (MAPS) data provided by the National Oceanic and Atmospheric Administration (NOAA), were compared at the location of the ASTER site with the in situ data. In particular the wind, temperature, and humidity at the lowest model grid point (~36 m AGL) and the fluxes could be compared with direct observations each hour for a 24-hour period. The model was nested down to 20 and 6.67 km around the ASTER site for this experiment, and results will be shown from the 6.67-km grid points nearest the ASTER site.

This work is presented in more detail in Oncley and Dudhia.[(a)] The model set-up is described in a companion paper (Dudhia) in this volume.

Cases

Four cases from northeast Kansas were chosen for study during the STORM-FEST92 experiment.

- February 21, Julian Day (JD) 52. A warm front aligned NE-SW moves north through Kansas during the first 12 hours, then becomes stationary; initially cold then mild temperatures.

(a) Oncley, S. P., and J. Dudhia. Evaluation of surface fluxes from MM5 using observations. Submitted to *J. Atmos. Sci.*

- February 27, JD 58. Weak W to NW surface flow and little thermal advection during the day; mild conditions.
- March 1, JD 61. Weak SW to S surface flow and little thermal advection; mild conditions.
- March 10, JD 70. N to NW flow behind a cold front, becoming S later as another system approaches from the west; cold conditions getting milder.

Figure 1 shows sea-level pressure and low-level air temperature at 12 hours of the JD 61 simulation on the 20-km domain. The 6.67-km domain is delineated in the figure where the ASTER site is marked (A).

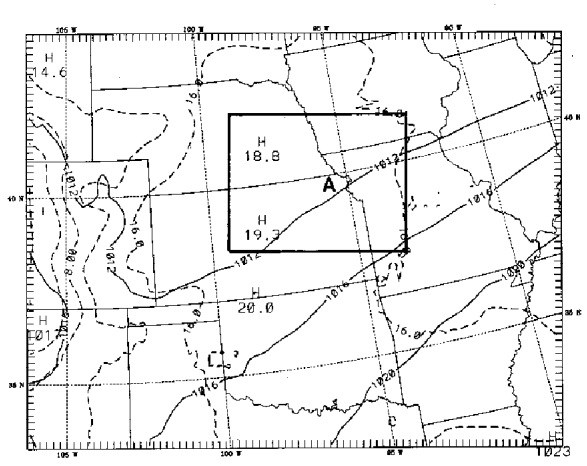

Figure 1. Sea-level pressure (solid), surface layer air temperature (dashed), JD 61 simulation. Contour 4 mb and 4 C, box shows 6.67-km domain, A marks ASTER site.

Model Parameterizations of Fluxes

The surface fluxes are based on similarity theory accounting for the stability of the surface layer. First some eddy perturbation quantities are defined,

$$u_* = \frac{kU}{ln(z/z_0) - \varphi_m} \quad (1)$$

$$\theta_* = \frac{k(\theta - \theta_0)}{ln(z/z_0) - \varphi_h} \quad (2)$$

$$q_* = \frac{M\,k(Q_{s0} - Q)}{ln\left(\frac{ku_*z}{K_a} + \frac{z}{z_l}\right) - \varphi_h} \quad (3)$$

where U, θ, Q are the wind, potential temperature and moisture at the lowest model level; θ_0, Q_{s0} are the potential temperature and saturation specific humidity at the ground; z_0, M are the roughness and moisture availability of the surface type φ_m, φ_h are corrections dependent on the stability, z_l = 1 cm, k = 0.4 K_a is the molecular diffusivity. Ground temperature is prognostic based upon the energy budget.

The fluxes are then given by u_*u_* for momentum, $u_*\theta_*$ for potential temperature, u_*q_* and for moisture.

Time Series of Rainfall, Soil Moisture, and Net Radiation

As seen in the time series of rainfall, soil moisture, and net radiation (Figure 2), during the period covering the four simulations (JD 52, 58, 61, 70, shaded columns in the figure), soil moisture drops gradually between rainfall events at JD 49 and JD 63. The net radiation is particularly high between JD 58 and JD 62, owing to clear skies; and the soil moisture reaches a minimum before JD 61. Julian Day 70 is just after a rainfall episode.

Results: Moisture Availability Test

The simulations for the four days were compared with observations at the grid points closest to the ASTER site using hourly model output. Generally the model was able to reproduce the observed time series of wind, temperature, and moisture well, but there were significant departures in one case.

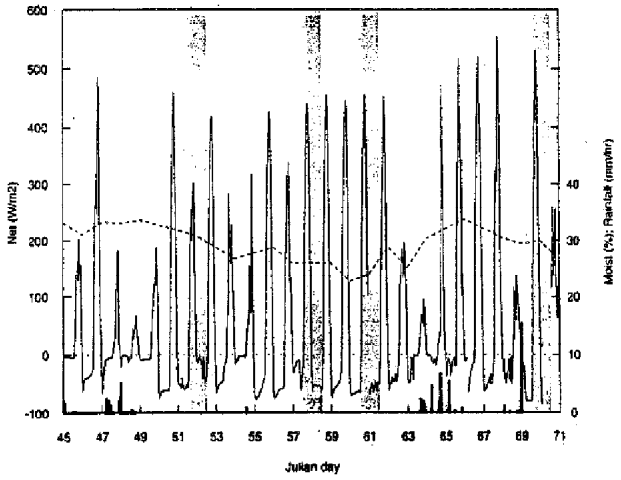

Figure 2. Time series of rainfall (histogram), soil moisture (dashed), and net radiation (solid) at the ASTER site between JD 45 (February 14) and JD 71 (March 11) 1992.

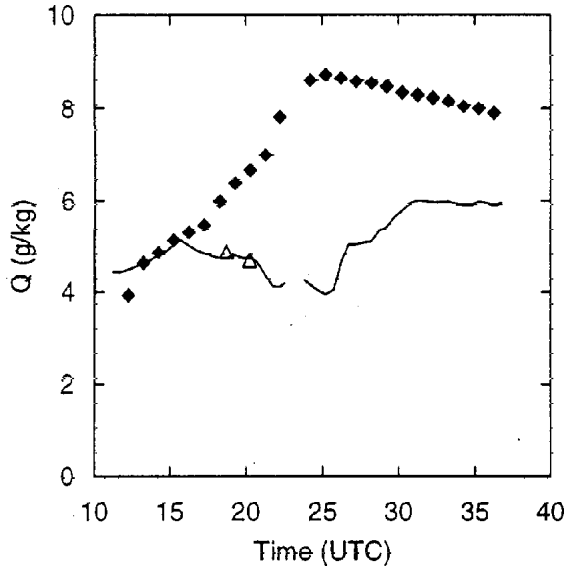

Figure 3a. JD 61, moisture at low levels from model with M = 0.6 (diamonds), surface observations (solid), and King Air (triangles).

The simulation of JD 61 was particularly inaccurate in the surface layer prediction of moisture and temperature, as can be seen from Figures 3a and 3b. The model over-moistens and under-heats the lowest atmospheric layer relative to the observed properties.

Comparison of the model fluxes against ASTER measurements shows that the error is due to incorrect local surface fluxes rather than large-scale advection, which is weak in this case. Figure 4 shows that the model fluxes are significantly higher than the ASTER measurement. The derived q^* from surface observations and Equation (3) using M = 0.6 is also high by a similar amount, showing that the model formulation, particularly for soil moisture, is inappropriate for this dry-soil case.

As shown in Figure 2, JD 61 is at the end of a significant dry spell with high net radiation, and it is likely that the true moisture availability of the soil is lower than the default value. Modifying the soil moisture availability from 0.6 to 0.1 produces a marked improvement, as shown in Figures 5a and 5b. The air temperature prediction near the ground is also improved because of the more realistic partitioning of latent and sensible heat fluxes.

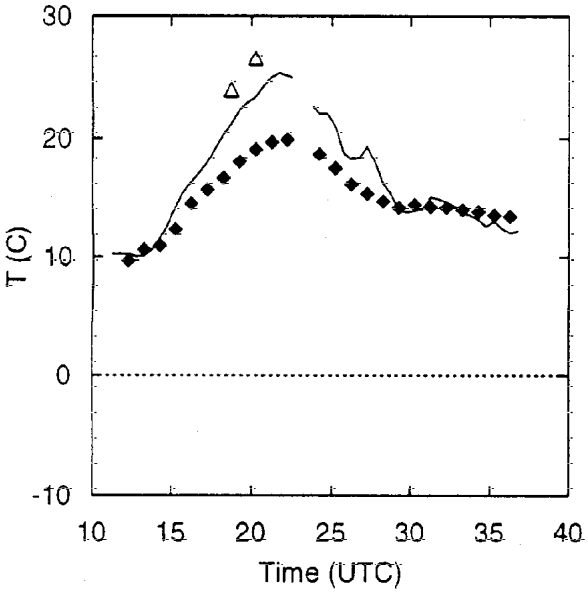

Figure 3b. JD 61, temperature at low levels from model with M = 0.6 (diamonds), surface observations (solid), and King Air (triangles).

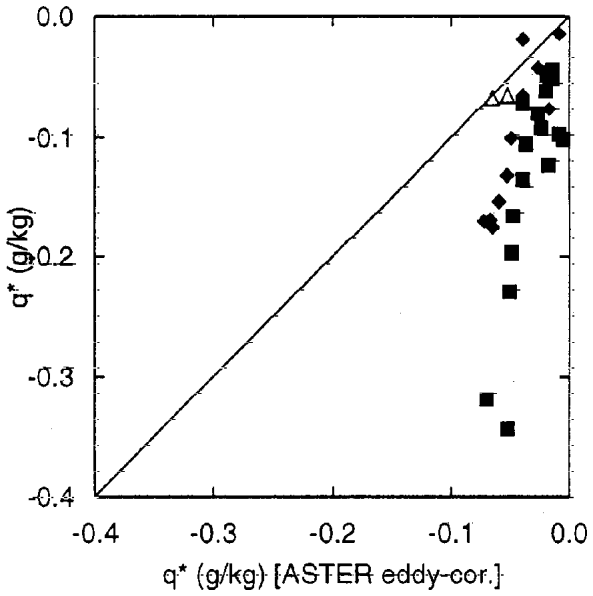

Figure 4. Comparison of *q** between model (diamonds), surface observation using Equation (3) (squares), King Air (triangles), and ASTER direct measurements.

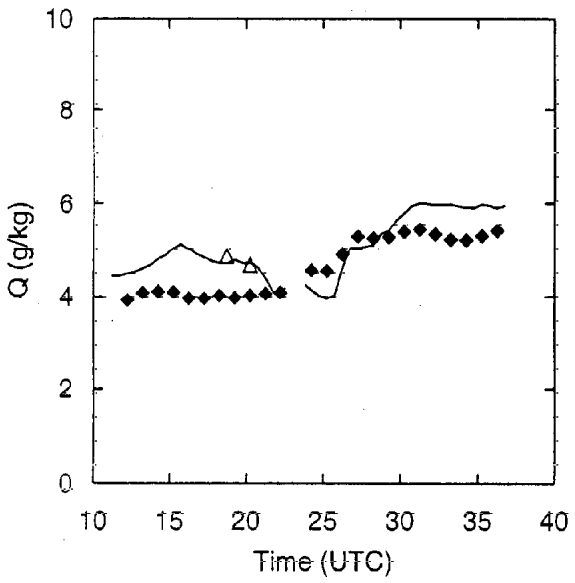

Figure 5a. JD 61, moisture at low levels from model with M = 0.1 (diamonds), surface observations (solid), and King Air (triangles).

Figure 6 shows that the correlation between model and observed *q** is also improved using M = 0.1.

Conclusions

Overall, the model representation of surface processes is good, given that it assigns surface properties based purely on land-use category apart from the ground temperature, which is a prognostic variable. The primary deficiency of this simplification, at least in the land-use category of agriculture, is the lack of soil moisture as a variable.

The results show that the default moisture availability (M = 0.6) can be much too high occasionally, and sometimes too low, depending upon the recent rainfall and cloud cover history of the area. A high value, in addition to causing overpredicted moisture fluxes, also leads to underprediction of sensible heat flux and hence air temperature.

Correction of *M* to a more appropriate value of 0.1 for dry soil improves both the air temperature and moisture prediction in the model.

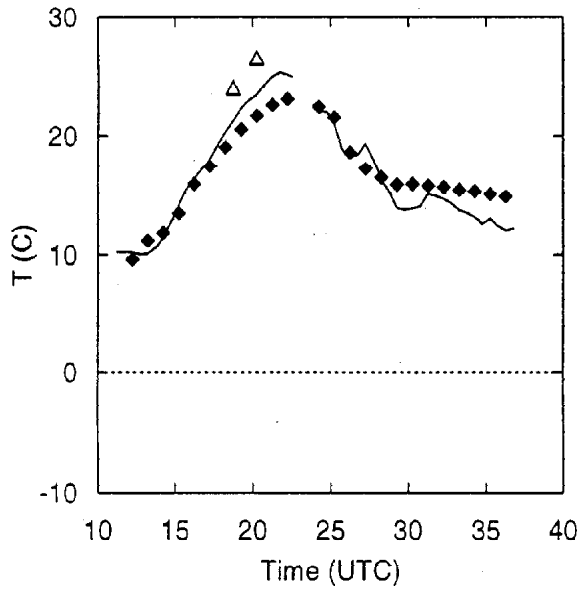

Figure 5b. JD 61, temperature at low levels from model with M = 0.1 (diamonds), surface observations (solid), and King Air (triangles).

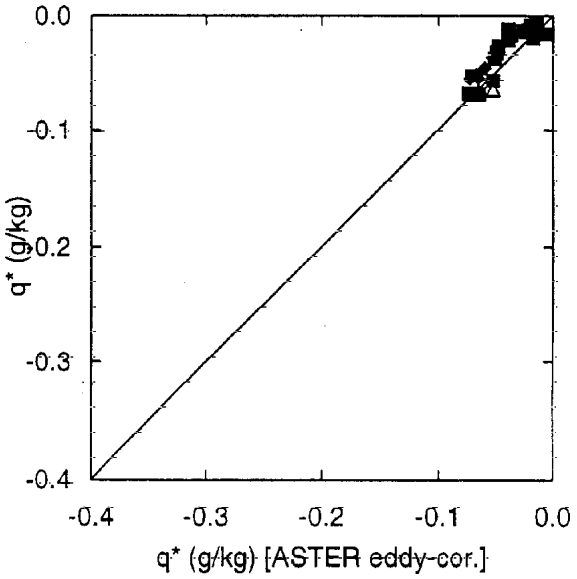

Figure 6. Comparison of *q** model (diamonds), surface observation using Equation (3) (squares), King Air (triangles), and ASTER direct measurements.

These results imply that soil moisture measurements should be an important part of a mesoscale data assimilation system. Alternatively, a method of estimating soil moisture based upon rainfall history and cloud cover history is required.

Acknowledgments

This work has been funded by the Department of Energy ARM Project under grant DEA105-90ER61070. Computing was carried out on the NCAR CRAY-YMP supported by the National Science Foundation and the Cray-3 supported by the Cray Computer Corporation.

References

Oncley, S., and J. Dudhia. 1993. Comparison of Mesoscale Model and Tower Measurements of Surface Fluxes During WISP91. *Proceedings of the Third Atmospheric Radiation Measurement (ARM) Science Team Meeting, Norman, Oklahoma, March 1993*, pp. 175-178. CONF-9303112. U.S. Department of Energy, Washington, D.C.